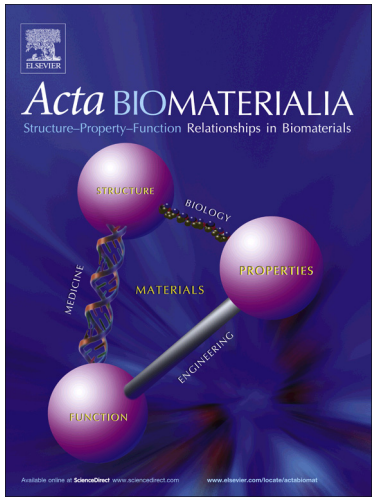

Adhesive free-standing multilayer films containing sulfated levan for biomedical applications

Tiago D. Gomes, Sofia G. Caridade, Maria P. Sousa, Sara Azevedo, Muhammed Y. Kandur, Ebru T. Öner, Natália M. Alves, João F. Mano

PII: S1742-7061(18)30038-2
DOI: https://doi.org/10.1016/j.actbio.2018.01.027
Reference: ACTBIO 5282

To appear in: *Acta Biomaterialia*

Received Date: 12 September 2017
Revised Date: 9 December 2017
Accepted Date: 18 January 2018

Please cite this article as: Gomes, T.D., Caridade, S.G., Sousa, M.P., Azevedo, S., Kandur, M.Y., Öner, E.T., Alves, N.M., Mano, J.F., Adhesive free-standing multilayer films containing sulfated levan for biomedical applications, *Acta Biomaterialia* (2018), doi: https://doi.org/10.1016/j.actbio.2018.01.027

Adhesive free-standing multilayer films containing sulfated levan for biomedical applications

Tiago D. Gomes[1,2,*], Sofia G. Caridade[1,2,3*&], Maria P. Sousa[1,2,3], Sara Azevedo[3], Muhammed Y. Kandur[1,2,4], Ebru T. Öner[4], Natália M. Alves[1,2], João F. Mano[1,2,3&]

[1] 3B's Research Group, Biomaterials, Biodegradables and Biomimetics, University of Minho, Headquarters of the European Institute of Excellence on Tissue Engineering and Regenerative Medicine, AvePark-Parque de Ciência e Tecnologia, 4805-017 Barco, Taipas, Guimarães, Portugal.

[2] ICVS/3B's, Associate PT Government Laboratory, Braga/Guimarães, Portugal.

[3] Current address: Department of Chemistry CICECO—Aveiro Institute of Materials University of Aveiro 3810-193 Aveiro (Portugal).

[4] IBSB, Department of Bioengineering, Marmara University, Istanbul, Turkey

* Co-first authors; these authors contributed equally.

[&]*Corresponding authors.* Address: Department of Chemistry, CICECO - Aveiro Institute of Materials; University of Aveiro, 3810-193 Aveiro, Portugal. TEL.: +351-234370733. Fax: +351-234401470. Email address (Sofia G. Caridade): sofiafi26@gmail.com. Email address(João F. Mano): jmano@ua.pt.

Abstract

This work is the first reporting the use of layer-by-layer to produce adhesive free-standing (FS) films fully produced using natural-based macromolecules: chitosan (CHI), alginate (ALG) and sulfated levan (L-S). The deposition conditions of the natural polymers were studied through zeta potential measurements and quartz crystal microbalance with dissipation monitoring analysis. The properties of the FS films were evaluated and compared with the control ones composed of only CHI and ALG in order to assess the influence of levan polysaccharide introduced in the multilayers. Tensile tests, dynamic mechanical analysis and single lap shear strength tests were performed to evaluate the mechanical properties of the prepared FS. The presence of L-S conferred both higher tensile strength and shear strength to the developed FS. The results showed an adhesion strength 4 times higher than the control (CHI/ALG) FS films demonstrating the adhesive character of the FS films containing L-S. Morphological and topography studies were carried out revealing that the crosslinking reaction granted the L-S based FS film with a higher roughness and surface homogeneity. Preliminary biological assays were performed by cultivating myoblasts cells on the surface of the produced FS. Both crosslinked and uncrosslinked FS films containing L-S were cytocompatible and myoconductive.

Keywords: Sulfated Levan; Free-standing membranes; Adhesiveness; Biomedical applications

Introduction

Suture has been the practice of choice for wound closure and bleeding control but they have many disadvantages such as, high infection rate, inconvenience in

handling, and concern over possible transmission of blood-borne disease through the use of needles. There is thus a need to overcome such drawbacks in which an easy method to repair or attach devices to tissues would be welcomed by surgeons. One of the goals of tissue engineering consists on the design and development of biocompatible tissue adhesives and sealants with high adhesion properties in order to face the actual adverse effects of the sutures [1, 2]. Several polymeric materials, either natural or synthetic [1-3], are being designed for the conception of materials with adhesive properties. Although several improvements are being done, many challenges remain to be achieved. For instance, some adhesives can trigger allergic reactions in some patients, mainly the ones that are derived from bovine sources. Other issues are related with long preparation time, inefficacy in high pressure bleeding, low stability in aqueous environment, others generate heat during polymerization having concerns about their degradation products, they may lack required flexibility, some possess high swelling ratio which requires more caution when they are applied to closed spaces to avoid pressure buildup on surrounding tissues and some sealants perform better when applied to dry surfaces which is a limiting factor when wet tissue adhesion is required.

Nature gives us a wealth of resources that can be exploited for medical adhesives and sealants such as collagen, cellulose, fibrin and mussel adhesive proteins [4-8]. While the sea is a good source of natural bioadhesive materials, it is also possible to find other interesting materials through less conventional sources such as extremophilic environments as is the case of levan.

Levan is a fructan polymer composed of β(2→6)-linked fructose residues and it is one of the most widely distributed polysaccharides in nature. It is produced extracellularly from sucrose-based substrates by diverse microbial species that also include the first extremophilic levan producer halophilic bacterium *Halomonas*

smyrnensis AAD6T. Moreover, it is water-soluble, biocompatible, biodegradable, non-toxic and is capable of forming adhesive bonds with diverse substrates due to the large number of hydroxyl groups in its structure [9] and is being associated with many high value applications in medical, food, pharmaceutical, cosmetics and chemical industries. Among the different types of existing levan, sulfate-modified levan (L-S) has been reported to provide good experimental results as an anticoagulant as well as enhanced antioxidant and antitumor activity [10, 11]. Due such properties, this work aims to demonstrate its potential as a new adhesive device for biomedical applications. The proof-of-concept includes the assembly of L-S into multilayer films using the layer-by-layer technique (LbL). LbL is a versatile and easy-to-apply methods to produce either coatings or free-standing (FS) membranes in which several materials can be deposited sequentially through the spontaneous adsorption of various alternating materials [12, 13]. Among the different types of interaction that can be employed, this technique can be based on electrostatic attractions between oppositely charged molecules being a simple and versatile method to obtain multilayered structures [14]. Furthermore, this technique allows the production of robust nanostructured coatings on substrates with complex geometries and the use of harmful organic solvents is not needed. Importantly, depending on the applications envisaged, several materials can be selected. In particular, different authors have reported LbL strategies in order to have adhesive LbL films [15-22]. However, the production of FS membranes with adhesive proprerties using this technique has been scarce.

In this perspective, we intended to develop new FS films composed of chitosan (CHI), alginate (ALG) and sulfated derivative of *Halomonas* levan (L-S) in order to verify if L-S presents a viable option in LbL FS films development and if its usage can

grant enhanced properties, namely adhesiveness, mechanical and biological performance, when compared to the widely used FS CHI/ALG composition.

2. Experimental section

2.1. Materials

Medium molecular weight chitosan (CHI) was purchased from Sigma-Aldrich with a degree of deacetylation ranging from 75-85% and a viscosity of 0.2-0.8 Pa.s. Before its usage, CHI was purified by filtering steps and precipitation in water and ethanol, followed by freeze-drying. At low pH (<6.5), CHI is a positively charged polyelectrolyte. Sodium alginate (ALG) obtained from brown algae was also purchased from Sigma-Aldrich with a viscosity of 0.005-0.04 Pa.s and was used as received. Levan produced by *Halomonas smyrnensis* AAD6T cultures was sulfated with chlorosulfonic acid to obtain sulfated *Halomonas* levan (L-S) with a sulfation degree of 1.36 [23]. The reaction associated with the modification of L-S is show in scheme 1. Genipin was supplied from Waco Chemicals GmbH (Germany), ethanol from Fisher Chemical (USA) and sodium chloride (NaCl), phosphate buffered saline (PBS) and dimethyl sulfoxide (DMSO) were purchased from Sigma Aldrich.

For all experiments polyelectrolyte solutions were freshly prepared by dissolution in a sodium acetate buffer (0.1 M CH_3COOH; 0.15 M NaCl, pH 5.5, RT) using polymer concentrations of 0.3 mg/mL for the QCM-D experiments and 2.0 mg/mL for the production of the FS membranes.

Scheme 1

2.2. Zeta potential (ζ-potential) measurements

The ζ-potential of the polyelectrolytes was determined using a Zetasizer nano instrument (Malvern, United Kingdom) at 25 °C with a saline dispersion medium. An aqueous solution of each polymer was used at a concentration of 1 mg/mL and a pH value of 5.5.

2.3. Multilayer assembly monitoring using Quartz Crystal Microbalance with dissipation (QCM-D)

The formation of the multilayers was studied *in situ* using a QCM-D monitoring (Q-Sense E4 system, Q-Sense AB, Sweden). The QCM-D crystals were excited at 15, 25, 35, 45 and 55 MHz corresponding to the 3^{rd}, 5^{th},7^{th}, 9^{th} and 11^{th} overtones. The build-up of multilayer films composed of CHI and ALG is already well known [24]. In this work the QCM-D was used to analyse the influence of the inclusion of L-S in this system. The adsorption was studied using polyelectrolyte solutions at 0.3 mg/mL and at a constant flow rate of 50 µL/min using a deposition order of CHI/ALG/CHI/L-S repeated 5 times. Between each polyelectrolyte deposition, a rinsing solution of sodium acetate (0.1 M CH_3COOH; 0.15 M NaCl; pH 5.5) was introduced with an adsorption time of 5 min, while the polymer adsorption time was of 10 min each.

The films' viscoelastic properties were studied using the QTools software (Q-sense AB) which allowed to calculate the thickness of the multilayer films according to the Voigt model using a Simplex algorithm to find the minimum of the sum of the squares of the scaled errors between the experimental and model Δf and ΔD values [24]. The modelling was performed using the 7^{th}, 9^{th} and 11^{th} overtones. The solvent viscosity selected was 1 mPa.s and a film density of 1 g/cm^3. The solvent density was varied between values from 1000 to 1030 kg/m^3 in order to minimize the total error (χ^2).

2.4. Production of multilayer free-standing (FS) membranes

The production of the multilayer FS membranes was performed using the LbL methodology. This process was automatized using a home-made dipping robot. Polypropylene substrates were immersed in alternated polyelectrolyte solutions with a rinsing solution deposition between each polyelectrolyte. The rinsing solution used was a sodium acetate buffer (0.1 M CH_3COOH; 0.15 M NaCl; pH = 5.5) and the polymer solutions were used at a concentration of 2 mg/mL. Deposition time of the polyelectrolytes was 6 min and 4 min for the rinsing solution. Prior to film deposition, the substrates were cleaned with ethanol and rinsed thoroughly with water before being dried with a stream of nitrogen.

Two types of FS membranes were produced: Multilayer membranes containing CHI, ALG and L-S with a deposition order of CHI/ALG/CHI/L-S repeated for 100 cycles and multilayer membranes containing only CHI and ALG with the same number of layers, thereafter named as $(CHI/ALG/CHI/L\text{-}S)_{100}$ and $(CHI/ALG/CHI/ALG)_{100}$, respectively.

2.5. FS membrane crosslinking

$(CHI/ALG/CHI/L\text{-}S)_{100}$ membranes were also chemically crosslinked using genipin. A genipin solution (1 mg/mL) was prepared by dissolving the adequate amount of genipin into a dimethyl sulfoxide /sodium acetate buffer (0.15 M NaCl, pH 5.5) mixture (1:4 (v/v)). The crosslinking agent solution was incubated with membranes overnight at 37ºC. Afterwards, the membranes were extensively washed with ethanol and distilled water and dried. The FS membrane are named as X-Linked $(CHI/ALG/CHI/L\text{-}S)_{100}$.

2.6. X-Ray Spectroscopy (XPS)

The XPS analysis was performed using a Kratos Axis-Supra instrument. Due to the no conducting nature of the samples a co-axial electron neutralizer to minimize surface charging was used, which performed the neutralization by itself. The XPS measurements were carried out using monochromatic Al-Kα radiation (1486.6 eV). Photoelectrons were collected from a take-off angle of 90º relative to the sample surface. The measurement were carried out in a Constant Analyser Energy mode (CAE) with a 160 eV pass energy and 15 mA of emission current for survey spectra and 40 eV pass energy for high resolution spectra, using and emission current of 20 mA. Charge referencing was adjusted by setting the lower binding energy C1s photo peak at 285.0 eV C1s hydrocarbon peak. An electron flood gun was also employed to minimize surface charging (Charge compensation). The residual vacuum in the X-Ray analysis chamber was maintained at around 6.2×10^{-9}torr. The samples were fixed to the sample holder with double sided carbon tape. The C1s, O1s, N1s, S2p and survey spectra were recorded using a Kratos Axis-Supra instrument. Data analysis and atomic quantification were determined from the XPS peak areas using the ESCApe software supplied by the manufacturer Kratos Analytical.

2.7. Scanning electron microscopy (SEM)

The morphology of the produced membranes was studied using a JSM-6010LV SEM (JEOL, Japan) microscope, operating at 15 kV. The samples were coated before analysis with a gold layer, using an EM ACE600 (Leica Microsystems, Germany) sputter coater. To analyse the cross-sectional area, the membranes were dipped in liquid nitrogen until free fracture.

2.8. Atomic force microscopy (AFM)

A Dimension Icon AFM equipment (Bruker, France) with a spring constant of 0.06 N/m, operating in a ScanAsyst mode was used to study the topography and roughness of the FS membranes. The FS topography was studied with 512 x 512 pixels^2 at line rates of 1Hz. For suface roughness analysis, images with 10 x 10 μm^2 were obtained. Analysis of the AFM images was performed using NanoScope Analysis software and the root mean squared roughness (Rq) and average height (Ra) values were determined.

2.9. Water contact angles (WCA) measurement

Water contact angles of all surfaces were determined using a Goniometer equipment OCA 15+ (DataPhysics Instruments). The sessile drop method was applied in which a 5 μL drop of pure water was deposited on the sample surface by a syringe. As the water drop contacted the surface, images were acquired and analysed using the SCA 20 software.

2.10. Mechanical characterization and evaluation of the adhesive properties

The tensile behaviour of the FS films was evaluated using a universal mechanical testing equipment (Instron 5543, USA) equipped with a 1 kN load cell. The produced FS films were cut into rectangular shape, with approximately 5 mm width. Tensile tests were carried out with a gauge length of 10 mm and a loading speed of 1mm/min. After immersion overnight in a PBS solution, the cross-sectional area of the FS films was measured immediately before the tests, where the thickness was determined in three different regions of each sample using a micrometer (Mitutoyo, Japan). Resulting stress-strain curves allowed to determine the ultimate tensile strength (UTS), elongation at break, and Young's modulus of the multilayered FS films.

Dynamic mechanical analysis (DMA) was applied in order to study the mechanical/viscoelastic properties of the developed FS films. The FS strips were cut with ≈ 5 mm width and, prior to the DMA assays the samples were immersed in a PBS solution overnight. The geometry of the samples was then measured accurately for each sample where the thickness was determined in three different regions of each sample using a micrometer (Mitutoyo, Japan). The measurements were carried out using a Tritec 2000B DMA (Triton, UK) equipped with the tensile mode. FS films were clamped in the DMA apparatus with a gauge length of 10 mm and immersed in the PBS bath. After equilibration at 37°C, the DMA spectra were obtained during a frequency scan between 0.2 and 15 Hz. The experiments were performed under constant strain amplitude (50 μm) and a static pre-load of 1 N was applied during the tests to keep the sample tight. At least three specimens were tested for each condition with the same experimental settings.

The adhesive properties of the produced FS films were evaluated using a single lap shear strength test adapted from ASTM D1002 [25]. Rectangular samples (30 x 10 mm^2) were cut and overlapped in pairs with an overlapping area of 5 x 10 mm^2. Samples were then hydrated with a PBS solution and placed between firmly tight glass slides. After an immersion period of 24 h at 37 °C in a PBS solution, the glass slides were removed and the samples were tested using the universal mechanical testing equipment (Instron 5543) where each grip pulled the extremity of one of the overlapped samples. A tensile speed of 5 mm/min was used until sufficient stress was applied for membrane detachment. The resulting stress-strain curves allowed to determine the bonding strength of each type of FS film.

In addition to the measurement of the adhesion force, a non-quantitative test was applied to test the potential of bioadhesion of the FS films. Briefly, the membranes were

hydrated in PBS overnight and left in contact with a surface of a porcine bone for 3 days. At the end of that time, FS membranes were pulled out from the bone with the help of tweezers. This procedure was recorded by a video camera (Canon EOS 1200D).

2.11. Biological tests

2.11.1. Cell seeding preparation and cell culture

C2C12 myoblasts cell line (European Collection of Cell Cultures (ECCC), UK), was used to test the *in vitro* biocompatibility of the developed FS. Prior to cell culture, FS were subjected to a sterilization process with 70 % (v/v) ethanol, during 2 hours, and then removed and washed with sterile PBS. Two independent experiments were conducted for each condition and assay, with triplicates.

C2C12 cells were cultured in DMEM supplemented with 10% FBS and 1% of antibiotic/antimycotic (Sigma-Aldrich), at 37°C and 5% CO_2. When confluence was reached, the cells, at passage 6 to 8, were trypsinized, centrifuged and re-suspended in cell culture medium. Then the C2C12 were seeded at a density of 4.0 x 10^4 cells per cm^2 under static conditions in aliquots of 200 µl, on the top of the FS. After 4 hours, 800 µl of growth culture medium (GM) were added to each well. The myoblast- seeded FS were nourished with fresh GM every 2 days and maintained at 37°C and 5% CO_2 until the end of each experiment.

2.11.2. Viability and proliferation of C2C12 on the FS

The metabolic activity of the C2C12 seeded on the FS was measured using the 3-(4,5-dimethylthiazol-2-yl)-5-(3-carboxymethoxyphenyl)-2-(4-sulphophenyl)-2H tetrazolium (MTS colorimetric assay, Cell Titer 96 AQueous One Solution Cell Proliferation Assay, Promega, USA). At each time point (1, 5 and 7 days) the culture medium was removed and replaced with 500 µl of serum-free DMEM with 20% of MTS reagent (Promega, USA). After that, samples were protected from the light, incubated during 3 hours, at

37°C and 5% CO_2. The absorbance was measured with a microplate reader (BioTek, USA), at a wavelength of 490 nm. The negative control was considered as the background absorbance of serum-free medium. C2C12 relative viability was considered comparing the FS results with tissue culture polystyrene (TCPS) (3D Biomatrix, USA).

Cell proliferation of C2C12 seeded on the FS films was also investigated through the quantification of a fluorimetric double-stranded DNA (PicoGreen dsDNA kit; Life Technologies, UK). After each predetermined time-point (1, 5 and 7 days) the samples were washed with sterile PBS, transferred into eppendorfs containing 1 mL of ultra-pure water and incubated for 1 hour at 37 °C. Then, the samples were kept in a -80 °C freezer until testing. Samples were thawed and sonicated for 15 minutes and DNA standards ranging from 0 to 1.5 mg/ml were prepared. The PicoGreen® working solution was incubated with the recovered supernatant of each sample and standard for 10 minutes, in the dark at RT. A microplate reader (BioTek, USA) was used to measure the fluorescence, using a 485 and 528 nm as excitation and emission wavelengths, respectively. The fluorescence values were corrected for the fluorescence of the reagent blanks. The concentration of DNA was calculated against a standard curve obtained by the prepared DNA standards. At least triplicates were performed for each sample.

2.11.3. Focal adhesion formation and morphology of C2C12 on the FS

The morphology of the adherent cells on the FS was observed by fluorescent microscopy at days 1, 5 and 7. At each time point, the samples were washed with sterile PBS and fixed with 10% formalin in PBS solution; after 30 minutes the cells were permeabilized using 0.2 % (v/v) of Triton 100x in PBS, for 5 minutes, and the non-specific binding sites were blocked using 3%(w/v) BSA in PBS, for 30 minutes. Afterwards, fluorescein phalloidin (Sigma-Aldrich) at 1:150 in PBS, pH=7.4, was used to stain the F-actin of the cells and 4', 6-diami-dino-2-phenylindole, DAPI, (Sigma-

Aldrich) at 1:1000 in PBS, pH=7.4 to stain the nucleus of the cells. Between each stage, three washing steps were performed using sterile PBS. Fluorescence microscopy using a transmitted and reflected light microscope with apotome 2 (Axio Imager Z1m, Zeiss, Germany) was employed for imaging the C2C12 on the surface of the FS. The images were acquired and processed with the AxioVision software version: Zeiss2012 (Zeiss). The chosen micrographs were representative for each time point and condition. The formation of focal adhesions (FAs) after 4 hours was assessed on the surface of both produced uncrosslinked and crosslinked FS $(CHI/ALG/CHI/L\text{-}S)_{100}$. For that, adherent cells on the surface of the FS were labelled with an immunofluorescence antibody to vinculin (Abcam®, UK). Cell seeded FS were fixed with formalin 10% (Termo Fisher Scientific, USA), permeabilized with 1% Triton (Sigma Aldrich) for 5 minutes and the non-specific binding sites were blocked with 3% of BSA (Sigma Aldrich) for 1 hour. The samples were incubated at 4°C overnight with the primary antibody vinculin (1:400 in PBS) and then incubated with secondary donkey antibody anti-mouse Alexa Fluor 488 (Invitrogen™, USA) (1:1000 in PBS) for 1 hour at RT, in the dark. Finally, the cells were incubated with DAPI (1:1000 in PBS) at RT for 15 minutes. Prior to fluorescence microscopy, the samples were washed several times, and left in PBS overnight.

2.11.4. Myogenic Differentiation of the C2C12 seeded on the FS

After the achievement of 60% to 80% confluence of C2C12 seeded on the FS, GM was replaced by differentiation medium (DM) to induce myogenic differentiation. The DM was composed by DMEM supplemented with 2% of horse serum (HS) (Invitrogen ™) and 1% of antibiotic/antimycotic and was replaced every two days. After 7 days of differentiation, samples were washed with sterile PBS and fixed with 10% of formalin. After 30 minutes, they were washed 3 times and were then permeabilized with 1% of

Triton in PBS for 5 minutes and the non-specific binding was blocked with 3% of BSA in PBS for 1 hour. Between each step, the samples were washed 3 times with PBS. For immunofluorescence imaging, the cells were incubated with the primary antibody Troponin T (Acris Antibodies, Inc®, Germany), overnight at 4 °C, and then with the secondary goat antibody anti-mouse Alexa Fluor 488 (Invitrogen ™) for 1 hour at RT and in the dark. Finally, to stain the nuclei, the cells were incubated with DAPI for 15 minutes at RT and in the dark. Between each step, samples were extensively washed with PBS. As for the assessment of the morphology of the C2C12 on the surface of the FS, fluorescence microscopy was used using a transmitted and reflected light microscope with apotome 2 (Axio Imager Z1m, Zeiss, Germany). The images were acquired and processed with the AxioVision software version: Zeiss2012 (Zeiss). The chosen micrographs were representative for each time point and condition.

2.12. Statistical analysis

All data obtained from the characterization techniques was represented as average value ± standard deviation with at least three replicates for each test subject. For WCA and tensile tests data, namely ultimate tensile strength and strain at failure, a One-way ANOVA followed by Tukey's multiple comparison test was applied. Adhesion tests were analyzed using an unpaired t test with Welch's correction. For the cellular assays, Two-way ANOVA was used. Statistical significance of all tests was accepted for $p<0.05$ (*). All statistical analysis was performed using the software GraphPad Prism 6.0 and the correspondent statistical significance and standard deviation are represented in all graphs.

3. Results and discussion

3.1 Build-up of the multilayers

The L-S used in this work was produced using a Levan of microbial origin. The sulfation of the levan was performed by suspending the *Halomonas* levan in pyridine (C_5H_5N) onto which chlorosulfonic acid ($ClSO_3H$) was added (scheme 1). The degree of sulfation was then determined according to the Whistler and Spencer (1964) method [26]. The L-S used in this work was measured as having a degree of sulfation of 1.36. The L-S was also structurally characterized by FTIR and 2D-NMR as reported by Erginer *et al.* [23].

The zeta potential (ζ-potential) of CHI, ALG and L-S was measured before the study on the QCM-D. CHI exhibits a moderately high ζ-potential (26.67 ± 0.85 mV) that is due to the protonated amine groups under acidic state. Mirroring the ζ-potential of CHI, ALG possesses approximately the same degree of ζ-potential but negative (-29.83 ± 1.16 mV) due the presence of carboxylic groups. For L-S, although it has a much lower absolute value of ζ-potential than ALG, it also presents a negative value (-6.36 ± 0.52 mV) due to the sulfate groups in the levan chains. As the chosen technique to produce the films in this work is the LbL assembly, mainly based on electrostatic interactions, it is essential for the materials that will be used to have opposite ζ-potential [27]. Considering the ζ-potential values obtained, we hypothesise that CHI is able to interact with ALG and L-S through electrostatic interactions in order to form the desired multilayered structure.

QCM-D was used to monitor *in situ* the build-up of the polyelectrolytes. The buildup between CHI and L-S was first monitored. An effective film construction was observed (data not shown). As the motivation of this study was to evaluate the effect of L-S on the (CHI/ALG) films, the build-up between CHI, ALG and L-S was also

assessed. Figure 1A shows the variation of the normalized frequency (Δf/v) and dissipation (ΔD) of the 7th overtone corresponding to the deposition of 5 (CHI/ALG/CHI/L-S) tetralayers. The points depicted represent the state of frequency and dissipation after each material deposition which can be distinguished by the stepwise decrease in frequency and increase in dissipation. The decrease in frequency in each deposition step indicates that mass was adsorbed onto the gold-coated quartz crystals representing a successful deposition. Although L-S has a much lower value of ζ-potential thus presenting a lower adsorption than CHI and ALG, it is observable that the frequency also decreases upon the L-S adsorption. The results indicates that the L-S is effectively introduced in the multilayers. The dissipation (ΔD) values display a successive increase for each layer deposition which indicates that a non-rigid material is being adsorbed by the crystal surface.

Figure 1.

Modelling of the QCM-D data according to the Voigt model allowed further investigation into the multilayer structure properties such as thickness (Figure 1B), shear modulus and viscosity (Figure 1C). The thickness evolution of the build-up of the same 5 tetralayers is represented in Figure 1B, the constant increase in thickness also confirms the successful deposition of each polyelectrolyte. After the deposition of the 5 tetralayers the thickness was estimated to be 102 ± 3 nm. These values are based on the assumption that each layer has a uniform thickness. In the work of Silva *et al.* [28], (CHI/ALG) films revealed a thickness of *ca.* 250 nm for the same number of layers (20 layers) that is higher than the one obtained in this work where the concentration of the polyelectrolyte solutions were even lower than the ones used in this work (0.2 mg/mL

vs 0.3 mg/mL). This corroborates that the extent of deposition of L-S is lower than ALG.

Viscosity and shear modulus were also estimated using the same method – see Figure 1C. The build-up of the film provoked an increase in both viscosity and shear modulus reaching values of 7.4 mPa.s and 0.58 MPa for viscosity and shear modulus, respectively. Although the viscosity has a consistent value increase comparable to the thickness development, the shear modulus values have a more irregular increase. This increase in both properties is generally consistent with the knowledge that an increment of layers will cause higher viscous component and damping properties that characterize a "softer" film. Thus, the assembled multilayer film is not rigid and exhibits the characteristic viscoelastic behavior, which is typical of macromolecular systems [24].

QCM-D results reveal that L-S can be successfully included in (CHI/ALG) multilayered films to conceive a viscoelastic polymeric thin coating using the LbL approach. Thus, based on the such experiments, FS films were produced under the conditions described in the experimental section. Besides the $(CHI/ALG/CHI/ALG)_{100}$ and $(CHI/ALG/CHI/L\text{-}S)_{100}$ FS films, crosslinked - henceforth referred to as x-linked $(CHI/ALG/CHI/L\text{-}S)_{100}$ films - were also prepared. Genipin was used as the crosslinking agent [29-31] once it has been extensively investigated in the crosslinking of amine-containing polymers, such as CHI [32, 33]. In CHI-based materials this crosslinker acts through a nucleophilic attack of CHI C-2 to C-3 genipin, resulting in opening of the hydropyran ring and the formation of a nitrogen-irdoid which produce aromatic intermediates. Subsequent steps may involve radical induce polymerization that create genipin heterocyclic conjugates which can be exploited to further tailor the properties of the final construct. Additionally, the ester groups of genipin can react with amino

groups in CHI and secondary amide linkages can be established [34, 35]. This covalent crosslinking is permanent and presents high selectively [36, 37].

When CHI/ALG/CHI/L-S films are crosslinked with genipin, since ALG and L-S does not contain primary amines, genipin will give rise to semi interpenetrating polymer networks with free ALG and L-S chains entrapped inside crosslinked CHI multilayers, as previously reported in other multilayered systems [31, 38]. The chemical crosslinking with genipin leads to the formation of a permanent network (covalent bonds) by the nucleophilic attack of these small molecules in the amine groups of CHI [35]. A blue colour typical of the crosslinking reaction with genipin appeared some hours later on the x-linked $(CHI/ALG/CHI/L\text{-}S)_{100}$ FS films confirming the efficiency of the crosslinking process by simple visual inspection. The effect of crosslinking on the $(CHI/ALG/CHI/ALG)_{100}$ FS films was clearly reflected in properties, such as mechanical performance, adhesiveness, surface morphology and cell viability.

3.2 XPS analysis

The chemical composition of the prepared FS films was examined by XPS surface measurements. As expected, three main elements: carbon (C), oxygen (O) and nitrogen (N) were present in the survey spectrum of the prepared FS membranes. For the $(CHI/ALG/CHI/ALG)_{100}$ FS films a concentration of 64.69% C_{1s}, 31.62% O_{1s} and 3.69% N_{1s} was detected. For the $(CHI/ALG/CHI/L\text{-}S)_{100}$ FS films a concentration of 77.10% C_{1s}, 19.98% O_{1s} and 2.80% N_{1s} was detected as well as 0.12% S 2p that is due to the sulfur content of L-S.

3.3 Morphology of the free-standing films

The surface of the upper side (facing outward) and cross-section of the distinct FS films were evaluated by SEM (Figure 2). The SEM images show that the surface of

the prepared FS films presents some features with sizes in the order of 1-5 μm. No significant topographic differences were observed between the studied FS.

The cross-sections of all FS films also do not present visible differences evidencing a quite homogeneous and compact organization of the layers. However, it is possible to discern differences in the thickness between them. The $(CHI/ALG/CHI/ALG)_{100}$ were the thicker ones and presents a thickness of 193.25 ± 12.26 μm. The original and x-linked $(CHI/ALG/CHI/L\text{-}S)_{100}$ FS films present thicknesses of 54 ± 3.61 μm and 56.5 ± 1.6 μm, respectively. The results are consistent with the QCM-D results.

Figure 2.

The AFM technique was employed in order to study in more detail the surface topography and roughness of the upper side of the FS. Figure 3A, B and C show the representative images obtained using an analysis area of 10 x 10 μm^2 and the respective 3D representation of each type of FS. Analysis of the images obtained by AFM provided values of root mean squared roughness (Rq) (Figure 3D) and of average height (Ra) (Figure 3E).

Figure 3.

From both Rq and Ra results, the control FS films present the rougher surface. The introduction of L-S on the CHI/ALG system render the FS smooth, however, upon crosslinking, an increase in roughness ($p > 0.0001$) was verified when comparing both $(CHI/ALG/CHI/L\text{-}S)_{100}$ and X-linked $(CHI/ALG/CHI/L\text{-}S)_{100}$. Although it was not

possible to draw any conclusion by SEM about the roughness of the FS films, by AFM it was observed that the introduction of L-S rendered the surface smooth similarly to what was reported before on (CHI/Ph-levan) multilayer films where phosphonated derivative of *Halomonas* levan was used [20]. The crosslinking caused a significant increase in the roughness of the $(CHI/ALG/CHI/L\text{-}S)_{100}$ as it has been reported in other crosslinking studies [29, 35, 39]. Such rough topography and increase of surface area could be advantageous for cell adhesion [40].

3.4 Wettability

The wettability of the developed FS films was analysed by water contact angle (WCA) measurements. These results are displayed in Figure 4, presenting the WCA of both sides of each FS produced. On the side in contact with the substrate during the LbL process (down side), it is possible to verify that no significant changes occurred (WCA $\approx 80^{o}$), when comparing all the FS films. This is explained by the presence of the same material layer, CHI, in the first layer. The X-linked $(CHI/ALG/CHI/L\text{-}S)_{100}$ showed a significantly higher WCA than the uncrosslinked FS film. It is easily observable that the L-S has a more hydrophilic behaviour than ALG or CHI resulting in a much lower WCA in the $(CHI/ALG/CHI/L\text{-}S)_{100}$. The hydrophilicity of the $(CHI/ALG/CHI/L\text{-}S)_{100}$ FS film is considerably decreased in the crosslinked FS film both WCA continues to be lower than in the $(CHI/ALG/CHI/ALG)_{100}$.

Figure 4.

3.5 Mechanical behaviour

Tensile tests allowed to study the elastic (Young) modulus, ultimate tensile strength (UTS) and strain at failure (ε) of the FS films – see Figure 5. The mechanical

tests demonstrated that the X-linked $(CHI/ALG/CHI/L\text{-}S)_{100}$ FS films possess a Young modulus of 31.52 ± 1.08 MPa being the stiffer films, followed by the $(CHI/ALG/CHI/L\text{-}S)_{100}$ FS films that have a Young modulus value of 17.77 ± 1.09 MPa. The softer FS films are the $(CHI/ALG/CHI/ALG)_{100}$.ones that have an elastic modulus of 7.45 ± 0.60 MPa meaning that the inclusion of L-S provoked an increase in the rigidity on the produced FS films. Also, these tests revealed that both the uncrosslinked and the crosslinked $(CHI/ALG/CHI/L\text{-}S)_{100}$ FS have a much higher UTS (3.80 ± 0.75 MPa and 3.73 ± 0.3 MPa, respectively) than the $(CHI/ALG/CHI/ALG)_{100}$ FS (1.25 ± 0.47 MPa). Regarding the strain at failure, the $(CHI/ALG/CHI/ALG)_{100}$ FS films have a deformation slightly lower value than the $(CHI/ALG/CHI/L\text{-}S)_{100}$ films. On the other hand, the X-linked $(CHI/ALG/CHI/L\text{-}S)_{100}$ have a much lower deformation which is caused by the higher structural stiffness granted by the crosslinking reaction as reported by other works [28, 41].

Analysing these values, it is possible to conclude that the presence of L-S results in a higher tensile resistance. It is also observable that the crosslinking on the FS with L-S does not appear to confer any considerable difference in terms of UTS, however it causes a significant decrease in strain at failure ($p < 0.0001$).

Figure 5.

DMA tests performed with the FS films allowed to evaluate their viscoelastic behaviour – see Figure 6. The storage modulus (*E'*) values show a consistent increase with frequency in all samples (Figure 6A). $(CHI/ALG/CHI/L\text{-}S)_{100}$ have an increased stiffness, with *E'* values that are approximately 2 times higher than the $(CHI/ALG/CHI/ALG)_{100}$ FS. As it was expected, the X-linked $(CHI/ALG/CHI/L\text{-}S)_{100}$

presents an even higher stiffness, as the *E'* values are more than 3 times higher than the uncrosslinked $(CHI/ALG/CHI/L\text{-}S)_{100}$ FS films. These values are in agreement with the behaviour observed in the tensile tests for the Young modulus. Moreover, such results are also consistent with dependent water uptake results in which $(CHI/ALG/CHI/ALG)_{100}$ and $(CHI/ALG/CHI/L\text{-}S)_{100}$ FS films presented a water uptake of 175 % and of 125 %, respectively (data not shown). Such behaviour has been already reported by other works where it was found that the mechanical properties of CHI membranes were influenced by their hydration levels [42-44].

As tan δ represents the ratio between the elastic and viscous behaviour of a material, it provides insight into the viscoelastic behaviour of the sample. Tan δ values (Figure 6B) are similar between the different studied FS. A general decrease with frequency was observed but no signs of the presence of relaxation processes could be detected. The X-linked $(CHI/ALG/CHI/L\text{-}S)_{100}$ present the lowest values of tan δ possessing lower dissipative properties than the other produced FS, which can be related to its higher crosslinking degree [45].

Considering that the tan δ values of all FS films present a value between 0.15 and 0.3 we can safely assume that these FS have a viscoelastic behaviour as it would be expected from a structure composed by natural polymers having the ability to absorb water.

Figure 6.

Previous studies have indicated that levan may present good adhesive properties mostly due to the presence of hydroxyl groups in its constitution [9, 20, 46, 47]. In order to study the adhesiveness of the films, they were subjected to lap shear strength tests

where the FS films were put in close contact through overlapping. In the case of the $(CHI/ALG/CHI/ALG)_{100}$ FS, the CHI side was overlapped with ALG side and, for the FS with L-S, the CHI side was put into contact with the L-S side. Figure 7 represents the average shear strength necessary to detach two FS of the same type of formulation. $(CHI/ALG/CHI/L\text{-}S)_{100}$ required a lap shear strength 4 times higher than the $(CHI/ALG/CHI/ALG)_{100}$ FS films. From these results, it is possible to confirm that the introduction of L-S contributes significantly to a higher adhesion strength. Some studies already investigated the lap shear strength necessary to separate two LbL films by using adhesive materials on the constitution of the multilayer films. For instance, (CHI/phosphonate-derivatized levan, Ph-levan) films revealed an increased adhesiveness compared to the (CHI/ALG), where an adhesive strength of 2.5 MPa and 0.9 MPa was verified for the films containing Ph-levan and for (CHI/ALG), respectively [20]. Neto *et al*. [21] found a higher adhesive strength (2.32 MPa) for multilayer films made of CHI and dopamine-modified hyaluronic acid (CHI/HA-DN) in comparison to (CHI/HA) films (0.75 MPa) confirmed also in high-throughput tests [22]. Multilayer films containing CHI, HA-DN and silver doped bioactive glass nanoparticles (AgBG) were produced where several combinations of the materials were used on the production of the multilayer films [48]. The films with the $[CHT/HA–DN/CHT/AgBG]_5$ + [CHT/HA–DN] sequence were the ones possessing the higher adhesiveness (around 1 MPa). Such studies reported lap closed with the ones reported in this work, but it should be noticed that such multilayered films were produced over glass slides and the overlapping was done immediately after film construction. In this work, the lap shear strength experiments were performed in FS films, meaning that the multilayers films were prepared and detached from their substrate just by letting them dry. Afterwards, the overlapping was done by rehydrating the FS. This could be an advantage since the

adhesiveness is not lost upon drying. Similar experiments [38] were performed with (CHI/ALG) FS membranes where adhesiveness was only verified when the FS films were immersed in a calcium chloride solution promoting a calcium-induced adhesion process. In this work, adhesiveness of the FS films occurred just by using PBS. Other adhesive materials have been proposed [49, 50] and some of them are already been used in clinical practice [51, 52] but they have less adhesive strength. Other evidence of the adhesion ability of the $(CHI/ALG/CHI/L\text{-}S)_{100}$ was given by a qualitative test, on which the membranes were attached on the surface of a porcine bone during 3 days, followed by its removal. It was observed that the $(CHI/ALG/CHI/L\text{-}S)_{100}$ FS films were more hard to pull out from the bone than the $(CHI/ALG/CHI/ALG)_{100}$ ones (see video recording). Thus, the $(CHI/ALG/CHI/L\text{-}S)_{100}$ with enhanced adhesive character could be used in biomedical applications where strong adhesiveness is required.

Figure 7.

3.6 Biological tests

The uncrosslinked (CHI/ALG) system has relatively low cell adhesion and proliferation on both fibroblasts [28, 53] and myoblast [54] cell lines. On the other hand, when crosslinked, the adhesion, proliferation [55] and even for differentiation [56] of cells on these FS films or even other similar ones were enhanced. In this work, *in-vitro* biological assays were performed on the $(CHI/ALG/CHI/L\text{-}S)_{100}$ and X-Linked $(CHI/ALG/CHI/L\text{-}S)_{100}$ FS films, as the main goal is to determine the influence that the L-S introduction could have on cell adhesion, proliferation and differentiation of C2C12 cells.

The cellular viability on the produced FS films are presented in Figure 8A. The cellular viability increased with increasing culturing time, suggesting good cell viability on the surfaces of the FS films. At day 1, significant differences were found for TCPS $p > 0.01$(**) and X-Linked (CHI/ALG/CHI/L-S)$_{100}$ $p > 0.01$(**) in relation to the (CHI/ALG/CHI/L-S)$_{100}$ FS. At day 5, TCPS presented significant differences $p > 0.0001$(****) and $p > 0.05$(*) in relation to (CHI/ALG/CHI/L-S)$_{100}$ and X-Linked (CHI/ALG/CHI/L-S)$_{100}$, respectively. Regarding (CHI/ALG/CHI/L-S)$_{100}$ FS, at day 7 significant differences were found for X-Linked (CHI/ALG/CHI/L-S)$_{100}$ $p > 0.05$(*) and for TCPS $p > 0.0001$(****). Figure 8B shows the DNA quantification along the different times points (1, 5 and 7 days). Overall, an increase in cell proliferation was verified for all tested substrates, suggesting the non-cytotoxicity of the material with the continuous growth of the cells above the FS. During all experiments, significant differences $p > 0.0001$(****) were verified for all formulations tested in relation to latex, a negative control, indicating that cells interacted well with both FS membranes and TCPS. Comparing the produced FS films, significant differences $p > 0.0001$(****) were found at day 5 and day 7 for the X-Linked (CHI/ALG/CHI/L-S)$_{100}$ confirming that the genipin crosslinking plays an important role in cell adhesion and proliferation of muscle cells, by tailoring the stiffness of the membrane. Overall, DNA quantification results matched with the MTS assay results. They reinforce the good C2C12 viability when cultured on both types of FS membranes, as well as enhanced cellular functions for X-Linked (CHI/ALG/CHI/L-S)$_{100}$. The results are consistent with previous results showing that C2C12 depend on substrate stiffness [57-59]. Briefly, when in contact with the membranes, cells interact with the substrate, receiving a mechanical feedback. Soft materials usually impair cell adhesion and performance [60]; with genipin crosslinking, it was possible to increase the stiffness of the FS membranes and this way,

to increase the myoblasts adhesion. Similarly, Silva J. M. *et. al* [53] improved the cellular adhesion to chitosan/alginate freestanding membranes, by increasing the stiffness of the membranes through crosslinking with genipin.

DAPI-phalloidin staining was performed to understand how C2C12 cells adhered and which morphology they presented on the surface of the produced FS films - see Figure 8C. At day 1, the cells presented a round shape typical of the short culture period and started to adhere on the surface of the produced membranes (data not shown). After a period of 5 and 7 days of culture in GM, the C2C12 presented a spread morphology exhibiting well-defined actin stress in the peripheral as well as the interior regions of the cell (data shown for 5 days of culture). Since the material stiffness influences the cell adhesion, it would be expected that it also affects cell morphology. However, after 5 days in GM, C2C12 cells were spread either when cultured on $(CHI/ALG/CHI/L\text{-}S)_{100}$ or X-Linked $(CHI/ALG/CHI/L\text{-}S)_{100}$ membranes. As the chemistry of the surface has been also reported by having influence on the behaviour of different type of cells, we hypothesize that it overpassed the differences on the mechanical properties. In fact, previous investigations have suggested that among other chemical groups, cells cultured on sulfate groups-containing surfaces exhibit largest contact area and a more spread morphology [61].

The functional adhesion to the $(CHI/ALG/CHI/L\text{-}S)_{100}$ and X-Linked $(CHI/ALG/CHI/L\text{-}S)_{100}$ FS was evaluated by the expression of focal adhesion (FAs) proteins using an immunofluorescent staining for vinculin - see Figure 9, top panel. The interactions at the interface between cell and material happen through multiple FAs contact, which are crucial to adapt the cell response to exogeneous regulatory mitogenic signals. After 4 h of culture, it was possible to observe the presence of FAs with no specific distribution over the surface, in all formulations studied; although, it seems that

there was some cell aggregation on the $(CHI/ALG/CHI/L\text{-}S)_{100}$ FS while for the X-Linked $(CHI/ALG/CHI/L\text{-}S)_{100}$ FS the cells were individually dispersed all over the surface. This could be related with the effect of crosslinking. Among other, crosslinking strategies have been reported as a strategy to enhance adhesion and proliferation of cells. Ren K. *et. al.* [59] suggested that stiffer films were obtained when crosslinking poly(L-lysine)/hyaluronan films, enhancing the formation of C2C12 focal adhesions and proliferation. Genipin crosslinking of different multilayer systems can be used to increase cell adhesion [29, 53, 62]; otherwise these systems are almost non-cell adhesive.

Differentiation experiments were also performed on the produced FS films where the C2C12 were in DM up to a period of 7 days– see Figure 9 bottom panel. Interestingly, myotubes were formed on all produced FS even for the uncrosslinked $(CHI/ALG/CHI/L\text{-}S)_{100}$. Muscle cells are very dependent on substrate stiffness that have influence in their differentiation in which, generally, cells are not able to form myotubes on soft substrates [56-59]. However, by the results of the immunofluorescence for troponin T, it seems that crosslinked and non-crosslinked membranes allowed myogenic differentiation. We hypothesize that the presence of L-S could have influence on the differentiation of C2C12, as sulfated groups have influence on cell differentiation [63-65]. Indeed, sulfated polysaccharides have been reported to influence the expression of different genes related with cell differentiation; the mechanism behind this phenomenon is not totally clear yet [66, 67]. Still, the intensity of troponin T immunofluorescence seemed higher and the formed myotubes appeared more elongated for cells seeded on X-Linked $(CHI/ALG/CHI/L\text{-}S)_{100}$ FS, which could be a result of the higher stiffness of these substrates. Ren K. *et. al.* [68] showed that stiffer polymer-based multilayer films

promotes the formation of more elongated and thin striated myotubes than soft substrates.

Overall, the developed FS could promote and control specific cellular responses through cell-material interactions. The preliminary biological assays indicate that the produced FS films are cytocompatible and able to allow myogenic differentiation.

Figure 8.

Figure 9.

Conclusions

The potential of FS films made of CHI and ALG are well known. In order to improve their potential L-S was included in their constitution. Free-standing membranes based on chitosan, alginate and sulfated levan were successfully produced using the LbL method, proving that sulfated levan is a suitable polyelectrolyte for such type of polyssacharide-based nanostructured multilayer films. The introduction of sulfated levan enabled the production of free-standing membranes with enhanced mechanical properties that required a higher tensile stress in order to rupture and a higher shear strength for detachment when compared to the widely used control membranes composed of chitosan and alginate. Moreover, such free-standing were myoconductive even in the absence of crosslinking. The crosslinking of the FS sulfated levan-containing films with genipin proved to improve their properties, granting a higher stiffness and surface roughness which in turn provided a higher mechanical resistance and enhanced cell viability and proliferation.

Finally, taking into account all the results, it is possible to conclude that the $(CHI/ALG/CHI/L\text{-}S)_{100}$ membranes that were developed in this study possess suitable conditions for distinct applications in the biomedical field, such as biological adhesives and for cardiac tissue engineering applications.

Acknowledgements

The authors acknowledge the Portuguese Foundation for Science and Technology (FCT) to financially supported this work through the scholarships SFRH/BPD/96797/2013 granted to Sofia G. Caridade and SFRH/BD/97606/2013 granted to Maria P. Sousa.

This work was also supported by the COST Action CA15216 from H2020.

References

[1] Mehdizadeh M, Yang J. Design Strategies and Applications of Tissue Bioadhesives. Macromol Biosci 2013;13:271-88.

[2] Ghobril C, Grinstaff MW. The chemistry and engineering of polymeric hydrogel adhesives for wound closure: a tutorial. Chem Soc Rev 2015;44:1820-35.

[3] Imam SH, Bilbao-Sainz C, Chiou BS, Glenn GM, Orts WJ. Biobased adhesives, gums, emulsions, and binders: current trends and future prospects. J Adhes Sci Technol 2013;27:1972-97.

[4] Spotnitz WD, Burks S. Hemostats, sealants, and adhesives III: a new update as well as cost and regulatory considerations for components of the surgical toolbox. Transfusion 2012;52:2243.

[5] Brubaker CE, Kissler H, Wang L-J, Kaufman DB, Messersmith PB. Biological performance of mussel-inspired adhesive in extrahepatic islet transplantation. Biomaterials 2010;31:420.

[6] Cheneler D, Bowen J. Degradation of polymer films. Soft Matter 2013;9:344.

[7] Waite JH, Tanzer ML. Polyphenolic Substance of Mytilus edulis: Novel Adhesive Containing L-Dopa and Hydroxyproline. Science 1981;212:1038.

[8] Lee Y, Lee H, Kim YB, Kim J, Hyeon T, Park H, Messersmith PB, Park TG. Bioinspired Surface Immobilization of Hyaluronic Acid on Monodisperse Magnetite Nanocrystals for Targeted Cancer Imaging. Adv Mater 2008;20:4154-7.

[9] Öner ET, Hernández L, Combie J. Review of Levan polysaccharide: From a century of past experiences to future prospects. Biotechnol Adv 2016;34:827-44.

[10] Akçay A. Investigations of Sulfate-Modified Levan Polysaccharides and their Bioactivity: Marmara University; 2014.

[11] Abdel-Fattah AM, Gamal-Eldeen AM, Helmy WA, Esawy MA. Antitumor and antioxidant activities of levan and its derivative from the isolate Bacillus subtilis NRC1aza. Carbohydr Polym 2012;89:314-22.

[12] Tang Z, Wang Y, Podsiadlo P, Kotov NA. Biomedical Applications of Layer- by- Layer Assembly: From Biomimetics to Tissue Engineering. Adv Mater 2006;18:3203-24.

[13] Costa RR, Mano JF. Polyelectrolyte multilayered assemblies in biomedical technologies. Chem Soc Rev 2014;43:3453-79.

[14] Borges J, Mano JF. Molecular Interactions Driving the Layer-by-Layer Assembly of Multilayers. Chem Rev 2014;114:8883-942.

[15] Chen D, Wu M, Chen J, Zhang C, Pan T, Zhang B, Tian H, Chen X, Sun J. Robust, Flexible, and Bioadhesive Free-Standing Films for the Co-Delivery of Antibiotics and Growth Factors. Langmuir 2014;30:13898-906.

[16] Fujie T, Kinoshita M, Shono S, Saito A, Okamura Y, Saitoh D, Takeoka S. Sealing effect of a polysaccharide nanosheet for murine cecal puncture. Surgery 2010;148:48-58.

[17] Fujie T, Matsutani N, Kinoshita M, Okamura Y, Saito A, Takeoka S. Adhesive, Flexible, and Robust Polysaccharide Nanosheets Integrated for Tissue- Defect Repair. Adv Funct Mater 2009;19:2560-8.

[18] Fujie T, Okamura Y, Takeoka S. Ubiquitous transference of a free-standing polysaccharide nanosheet with the development of a nano-adhesive plaster. Adv Mater 2007;19:3549-53.

[19] Gu Y, Zacharia NS. Self-Healing Actuating Adhesive Based on Polyelectrolyte Multilayers. Adv Funct Mater 2015;25:3785-92.

[20] Costa RR, Neto AI, Calgeris I, Correia CR, Pinho ACMd, Fonseca JC, Öner ET, Mano JF. Adhesive nanostructured multilayer films using a bacterial exopolysaccharide for biomedical applications. J Mater Chem B 2013;1:2367-74.

[21] Neto AI, Cibrão A, Correia CR, Carvalho RR, Luz G, Ferrer GG, Botelho G, Picart C, Alves NM, Mano JF. Nanostructured polymeric coatings based on chitosan and dopamine-modified hyaluronic acid for biomedical applications. Small 2014;10:2459-69.

[22] Neto AI, Vasconcelos NL, Oliveira SM, Ruiz-Molina D, Mano JF. High-Throughput Topographic, Mechanical, and Biological Screening of Multilayer Films Containing Mussel-Inspired Biopolymers. Adv Funct Mater 2016;26:2745-55.

[23] Erginer M, Akcay A, Coskunkan B, Morova T, Rende D, Bucak S, Baysal N, Ozisik R, Eroglu MS, Agirbasli M, Toksoy Oner E. Sulfated levan from Halomonas smyrnensis as a bioactive, heparin-mimetic glycan for cardiac tissue engineering applications. Carbohydr Polym 2016;149:289-96.

[24] Alves NM, Picart C, Mano JF. Self Assembling and Crosslinking of Polyelectrolyte Multilayer Films of Chitosan and Alginate Studied by QCM and IR Spectroscopy Macromol Biosci 2009;9:776-85.

[25] ASTM. Standard test method for: Apparent Shear Strenght of Single-Lap-Joint Adhesively Bonded Metal Specimens by Tension Loading (Metal - to - Metal). 1999.

[26] Whistler RL, Spencer WW. Sulfation. triethylamin-sulfur trioxide complex. Methods in carbohydrate chemistry IV: Academic Press; 1964. p. 297-8.

[27] Crespilho FN, Zucolotto V, Oliveira Jr. ON, Nart FC. Electrochemistry of Layer-by-Layer Films: a review. Int J Electrochem Sci 2006;1:194-214.

[28] Silva JM, Caridade SG, Oliveira NM, Reis RL, Mano JF. Chitosan–alginate multilayered films with gradients of physicochemical cues. J Mater Chem B 2015;3:4555-68.

[29] Hillberg AL, Holmes CA, Tabrizian M. Effect of genipin cross-linking on the cellular adhesion properties of layer-by-layer assembled polyelectrolyte films. Biomaterials 2009;30:4463-70.

[30] Chaubaroux C, Vrana E, Debry C, Schaaf P, Senger B, Voegel J-C, Haikel Y, Ringwald C, Hemmerlé J, Lavalle P, Boulmedais F. Collagen-Based Fibrillar Multilayer Films Cross-Linked by a Natural Agent. Biomacromolecules 2012;13:2128-35.

[31] Gaudière F, Morin-Grognet S, Bidault L, Lembré P, Pauthe E, Vannier J-P, Atmani H, Ladam G, Labat B. Genipin-Cross-Linked Layer-by-Layer Assemblies:

Biocompatible Microenvironments To Direct Bone Cell Fate. Biomacromolecules 2014;15:1602-11.

[32] Cui L, Jia J, Guo Y, Liu Y, Zhu P. Preparation and characterization of IPN hydrogels composed of chitosan and gelatin cross-linked by genipin. Carbohydr Polym 2014;99:31-8.

[33] Mekhail M, Jahan K, Tabrizian M. Genipin-crosslinked chitosan/poly-l-lysine gels promote fibroblast adhesion and proliferation. Carbohydr Polym 2014;108:91-8.

[34] Chen H, Ouyang W, Lawuyi B, Martoni C, Prakash S. Reaction of chitosan with genipin and its fluorogenic attributes for potential microcapsule membrane characterization. J Biomed Mater Res A 2005;75A:917-27.

[35] Gao L, Gan H, Meng Z, Gu R, Wu Z, Zhang L, Zhu X, Sun W, Li J, Zheng Y, Dou G. Effects of genipin cross-linking of chitosan hydrogels on cellular adhesion and viability. Colloids Surf B Biointerfaces 2014;117:398-405.

[36] Dragan ES. Design and applications of interpenetrating polymer network hydrogels. A review. Chem Eng J 2014;243:572-90.

[37] Reddy N, Reddy R, Jiang Q. Crosslinking biopolymers for biomedical applications. Trends Biotechnol 2015;33:362-9.

[38] Silva JM, Caridade SG, Reis RL, Mano JF. Polysaccharide-based freestanding multilayered membranes exhibiting reversible switchable properties. Soft Matter 2016;12:1200-9.

[39] Li Y-H, Cheng C-Y, Wang N-K, Tan H-Y, Tsai Y-J, Hsiao C-H, Ma DH-K, Yeh L-K. Characterization of the modified chitosan membrane cross-linked with genipin for the cultured corneal epithelial cells. Colloids Surf B Biointerfaces 2015;126:237-44.

[40] Chung T-W, Liu D-Z, Wang S-Y, Wang S-S. Enhancement of the growth of human endothelial cells by surface roughness at nanometer scale. Biomaterials 2003;24:4655-61.

[41] Silva JM, Duarte ARC, Custódio CA, Sher P, Neto AI, Pinho ACM, Fonseca J, Reis RL, Mano JF. Nanostructured Hollow Tubes Based on Chitosan and Alginate Multilayers. Adv Healthc Mater 2014;3:433-40.

[42] Mano JF. Viscoelastic properties of chitosan with different hydration degrees as studied by dynamic mechanical analysis. Macromol Biosci 2008;8:69-76.

[43] Silva RM, Silva GA, Coutinho OP, Mano JF, Reis RL. Preparation and characterisation in simulated body conditions of glutaraldehyde crosslinked chitosan membranes. J Mater Sci Mater Med 2004;15:1105-12.

[44] Caridade SG, Silva RMPd, Reis RL, Mano JF. Effect of solvent-dependent viscoelastic properties of chitosan membranes on the permeation of 2-phenylethanol. Carbohydr Polym 2009;75:651-9.

[45] Alves NM, Gómez Ribelles JL, Gómez Tejedor JA, Mano JF. Viscoelastic behaviour of polymethyl methacrylate networks with different crosslinking degrees. Macromolecules 2004:3735-44.

[46] Sima F, Mutlu EC, Eroglu MS, Sima LE, Serban N, Ristoscu C, Petrescu SM, Oner ET, Mihailescu IN. Levan Nanostructured Thin Films by MAPLE Assembling. Biomacromolecules 2011;12:2251-6.

[47] Donot F, Fontana A, Baccou JC, Schorr-Galindo S. Microbial exopolysaccharides: main examples of synthesis, excretion, genetics and extraction. Carbohydr Polym 2012;87:951.

[48] Carvalho AL, Vale AC, Sousa MP, Barbosa AM, Torrado E, Mano JF, Alves NM. Antibacterial bioadhesive layer-by-layer coatings for orthopedic applications. J Mater Chem B 2016;4:5385-93.

[49] Yamada K, Chen T, Kumar G, Vesnovsky O, Topoleski LD, Payne GF. Chitosan based water-resistant adhesive. Analogy to mussel glue. Biomacromolecules 2000;1:252.

[50] Yu M, Deming TJ. Synthetic Polypeptide Mimics of Marine Adhesives. Macromolecules 1998;31:4739–45.

[51] Elvin CM, Vuocolo T, Brownlee A, Sando L, Huson MG, Liyou NE, Stockwell PR, Lyons RE, Kim M, Edwards GA, Johnson G, McFarland GA, Ramshaw JA, Werkmeister JA. A highly elastic tissue sealant based on photopolymerised gelatin. Biomaterials 2010;31:8323-31.

[52] Murphy JL, Vollenweider L, Xu F, Lee BP. Adhesive performance of biomimetic adhesive-coated biologic scaffolds. Biomacromolecules 2010;11:2976-84.

[53] Silva JM, Duarte AR, Caridade SG, Picart C, Reis RL, Mano JF. Tailored Freestanding Multilayered Membranes Based on Chitosan and Alginate. Biomacromolecules 2014;15:3817-26.

[54] Caridade SG, Monge C, Gilde F, Boudou T, Mano JF, Picart C. Free-Standing Polyelectrolyte Membranes Made of Chitosan and Alginate. Biomacromolecules 2013;14:1653-60.

[55] Larkin AL, Davis RM, Rajagopalan P. Biocompatible, Detachable, and Free-Standing Polyelectrolyte Multilayer Films. Biomacromolecules 2010;11:2788-96.

[56] Caridade SG, Monge C, Almodóvar J, Guillot R, Lavaud J, Josserand V, Coll JL, Mano JF, Picart C. Myoconductive and osteoinductive free-standing polysaccharide membranes. Acta Biomater 2015;15:139-49.

[57] Engler AJ, Griffin MA, Sen S, Bönnemann CG, Sweeney HL, Discher DE. Myotubes differentiate optimally on substrates with tissue-like stiffness: pathological implications for soft or stiff microenvironments. J Cell Biol 2004;166:877-87.

[58] Gilbert PM, Havenstrite KL, Magnusson KEG, Sacco A, Leonardi NA, Kraft P, Nguyen NK, Thrun S, Lutolf MP, Blau HM. Substrate elasticity regulates skeletal muscle stem cell self-renewal in culture. Science (New York, NY) 2010;329:1078-81.

[59] Ren K, Crouzier T, Roy C, Picart C. Polyelectrolyte multilayer films of controlled stiffness modulate myoblast cells differentiation. Adv Funct Mater 2008;18:1378-89.

[60] Boudou T, Crouzier T, Ren K, Blin G, Picart C. Multiple Functionalities of Polyelectrolyte Multilayer Films: New Biomedical Applications. Adv Mater 2010;22:441-67.

[61] Ren Y-J, Zhang H, Huang H, Wang X-M, Zhou Z-Y, Cui F-Z, An Y-H. In vitro behavior of neural stem cells in response to different chemical functional groups. Biomaterials 2009;30:1036-44.

[62] Sousa M, Cleymand F, Mano J. Elastic chitosan/chondroitin sulfate multilayer membranes. Biomed Mater 2016;11:035008.

[63] Pisconti A, Bernet JD, Olwin BB. Syndecans in skeletal muscle development, regeneration and homeostasis. Muscles Ligaments Tendons J 2012;2:1-9.

[64] Ai X, Do A-T, Lozynska O, Kusche-Gullberg M, Lindahl U, Emerson CP. QSulf1 remodels the 6-O sulfation states of cell surface heparan sulfate proteoglycans to promote Wnt signaling. J Cell Biol 2003;162:341-51.

[65] Aggarwal N, Altgärde N, Svedhem S, Zhang K, Fischer S, Groth T. Effect of Molecular Composition of Heparin and Cellulose Sulfate on Multilayer Formation and Cell Response. Langmuir 2013;29:13853–64.

[66] Nakaoka R, Yamakoshi Y, Isama K, Tsuchiya T. Effects of surface chemistry prepared by self-assembled monolayers on osteoblast behavior. J. Biomed. Mater. Res. A 2010;94A:524-32.

[67] Nagira T, Nagahata-Ishiguro M, Tsuchiya T. Effects of sulfated hyaluronan on keratinocyte differentiation and Wnt and notch gene expression. Biomaterials 2007;28:844-50.

[68] Ren K, Crouzier T, Roy C, Picart C. Polyelectrolyte Multilayer Films of Controlled Stiffness Modulate Myoblast Cell Differentiation. Adv Funct Mater 2008;18:1378-89.

Figures

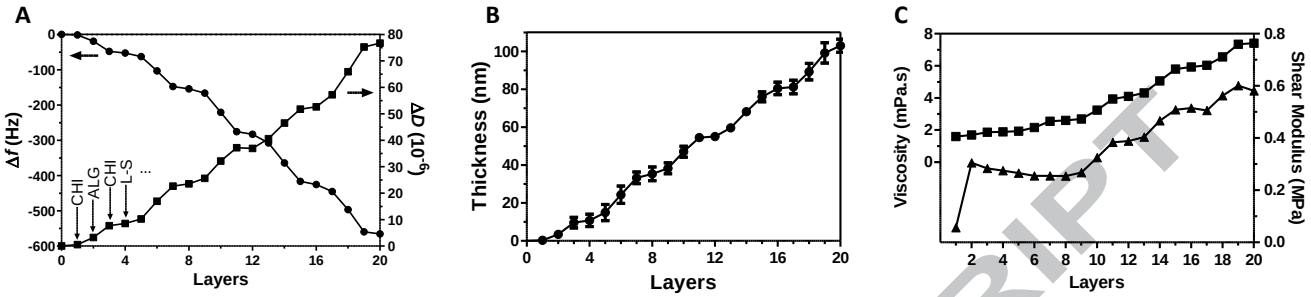

Figure 1. SG Caridade, *et al*

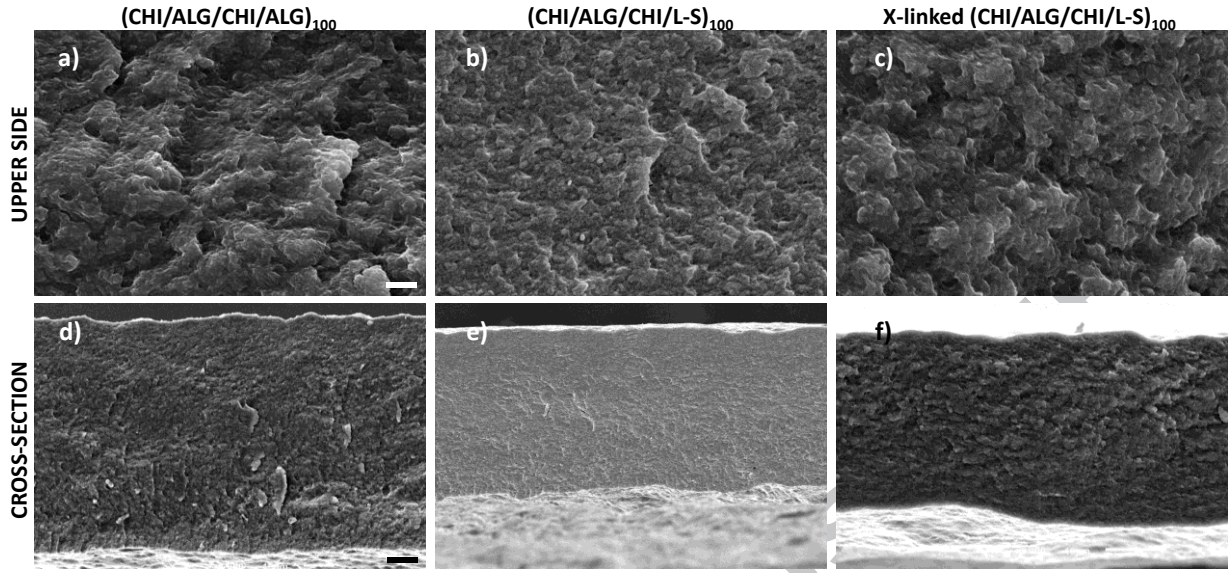

Figure 2. SG Caridade, *et al*

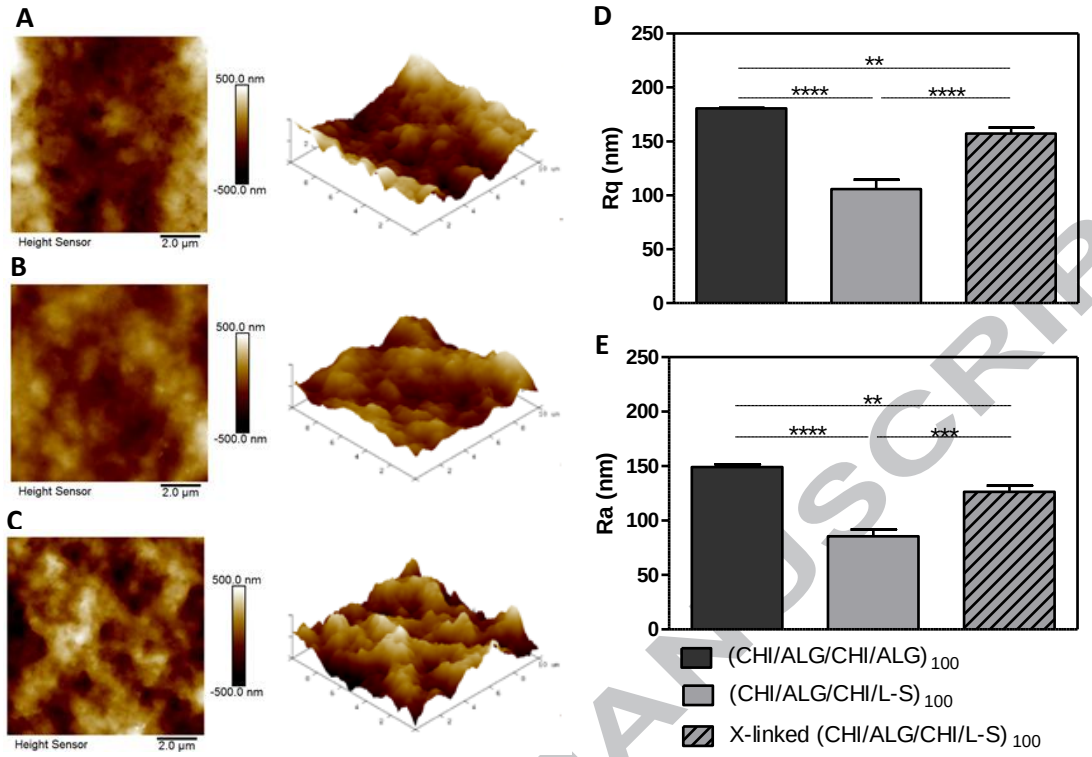

Figure 3. SG Caridade, *et al*

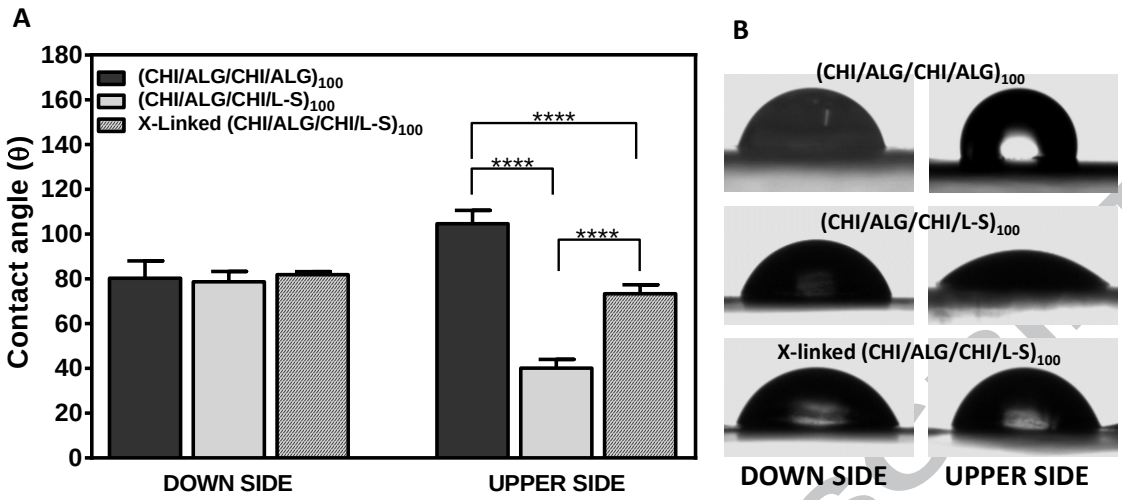

Figure 4. SG Caridade, *et al*

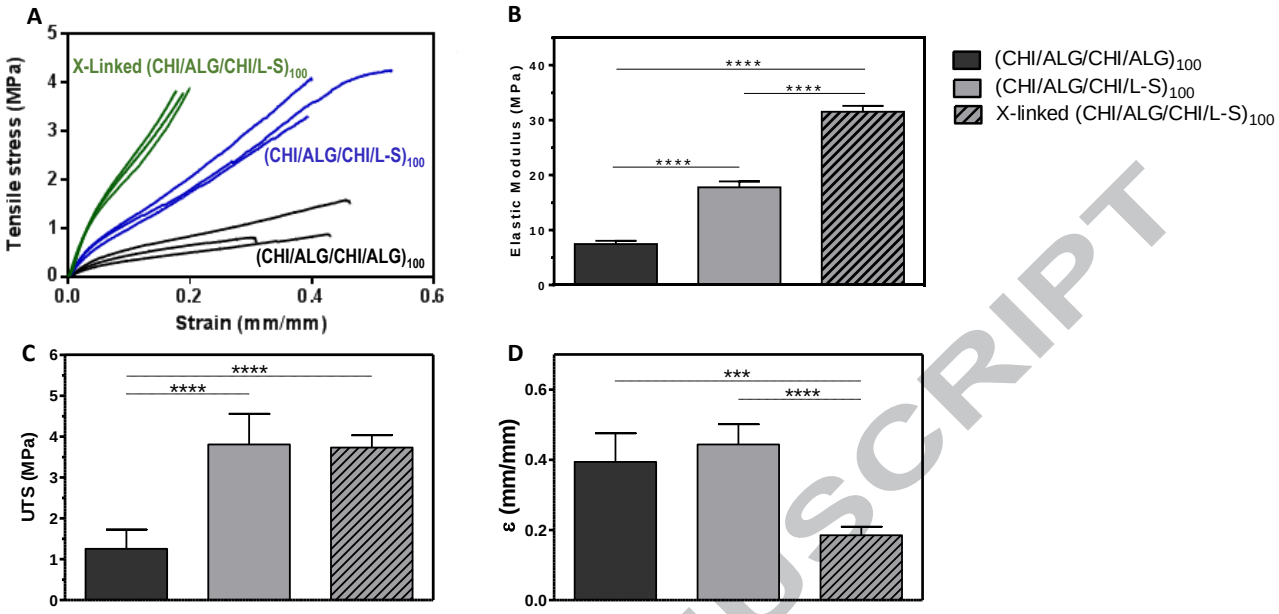

Figure 5. SG Caridade, *et al*

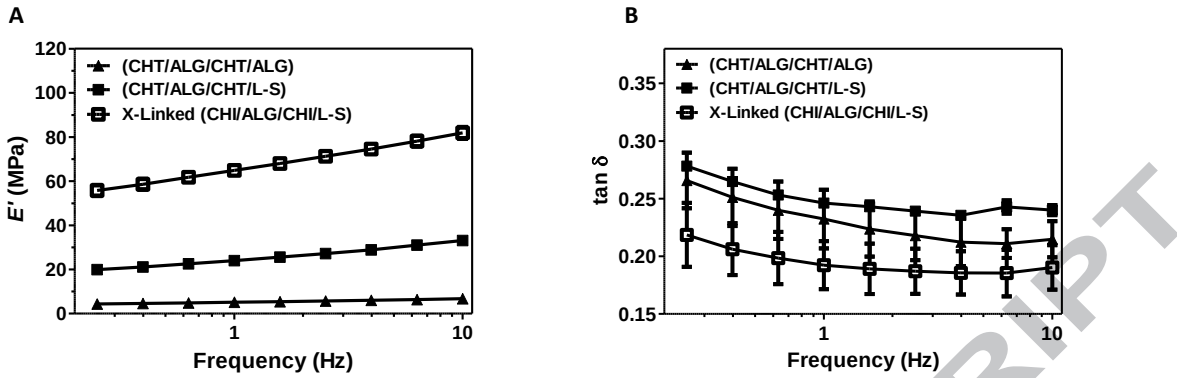

Figure 6. SG Caridade, *et al*

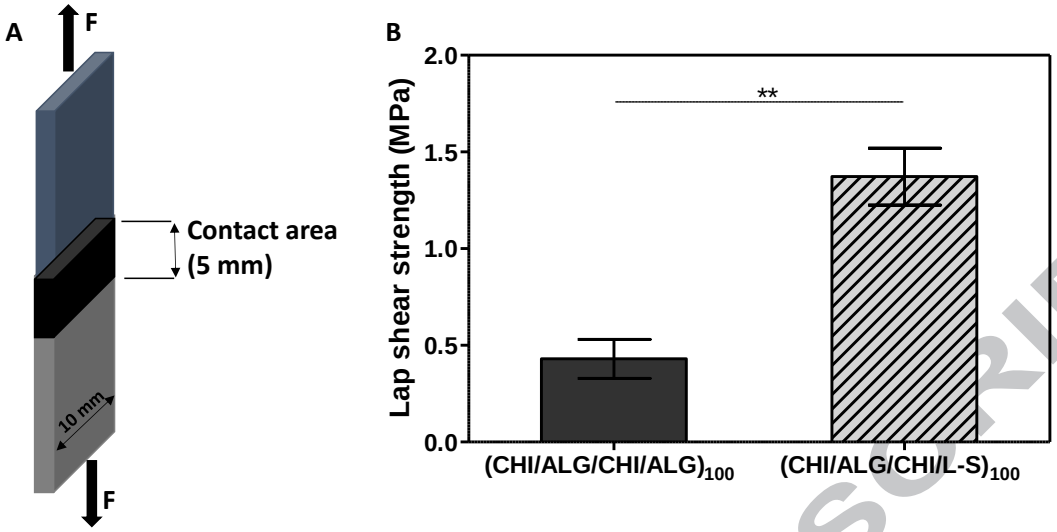

Figure 7. SG Caridade, *et al*

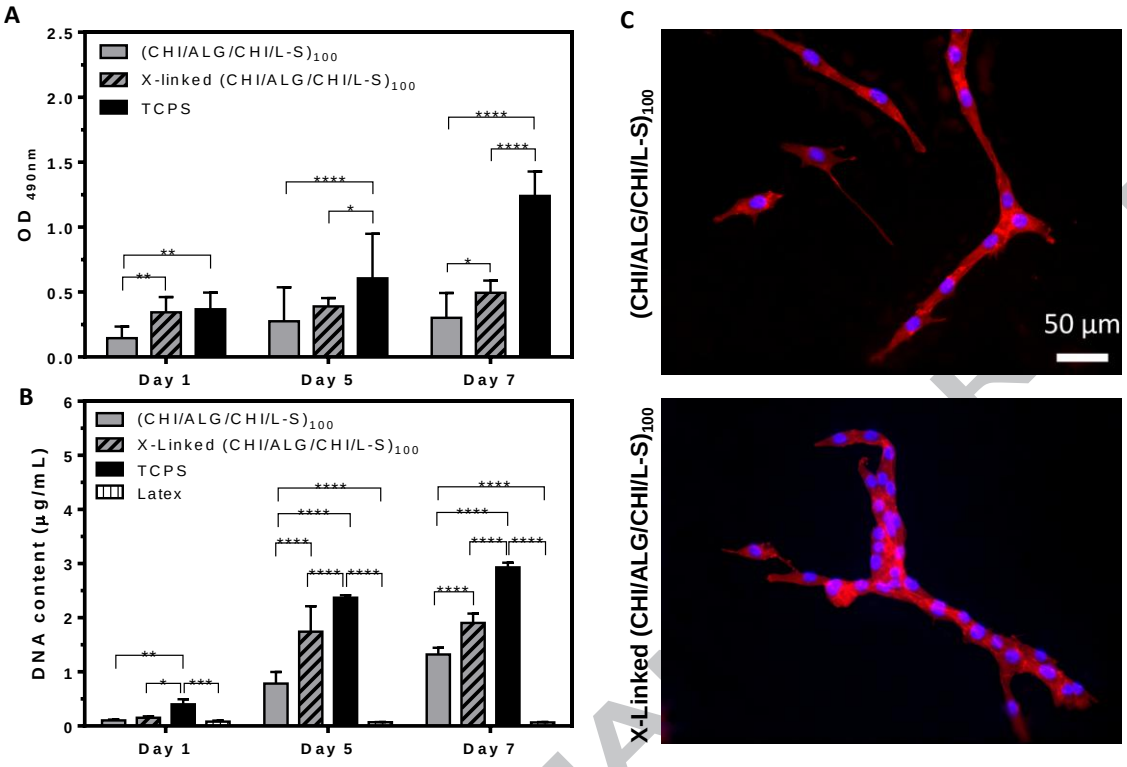

Figure 8. SG Caridade, *et al*

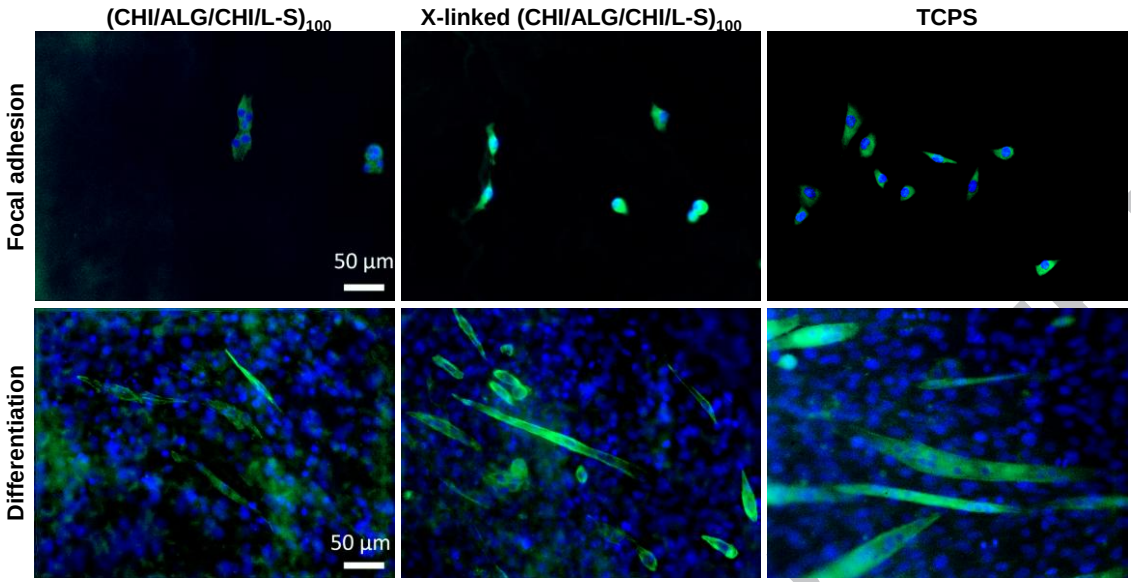

Figure 9. SG Caridade, *et al*

Scheme

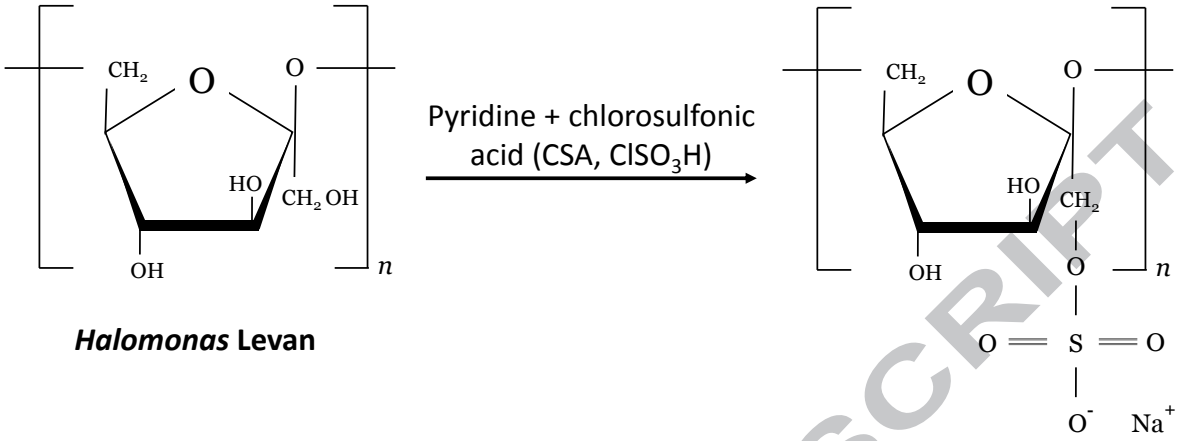

***Halomonas* Levan**

Sulfated *Halomonas* Levan

Scheme 1. SG Caridade, *et al*

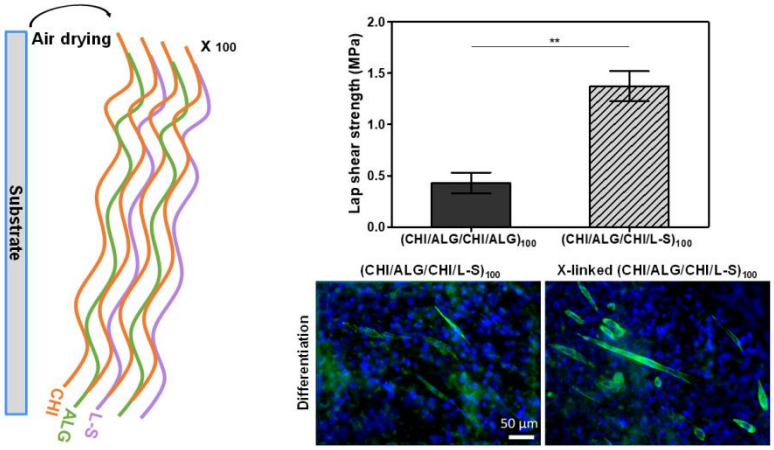

Statement of Significance

Sutures remain as the "gold standard" for wound closure and bleeding control; however they still have limitations such as, high infection rate, inconvenience in handling, and concern over possible transmission of blood-borne disease through the use of needles. One of the challenges of tissue engineering consist on the design and development of biocompatible tissue adhesives and sealants with high adhesion properties to repair or attach devices to tissues. In this work, the introduction of sulfated levan (L-S) on multilayered free-standing membranes was proposed to confer adhesive properties. Moreover, the films were myoconductive even in the absence of crosslinking just by the presence of L-S. This study provides a promising strategy to develop biological adhesives and for cardiac tissue engineering applications.